Review of rolling contact fatigue life calculation for oscillating bearings and recommendations for use, with examples for wind turbine bearings

Oliver Menck[1] and Matthias Stammler[1]

[1]Fraunhofer Institute for Wind Energy Systems IWES, Am Schleusengraben 22, 21029 Hamburg, Germany

Correspondence: Oliver Menck (oliver.menck@iwes.fraunhofer.de)

Abstract. In contrast to the multitude of calculation models in the literature for the calculation of rolling contact fatigue in rotating bearings, literature on oscillating bearings is sparse. This work summarizes the available literature on rolling contact fatigue in oscillating bearings. Publications which present various theoretical models are summarized and discussed. A number of errors and misunderstandings are highlighted, information gaps are filled, and common threads between publications are established. Recommendations are given for using the various models for any oscillating bearing in any industrial application. The applicability of these approaches to pitch and yaw bearings of wind turbines is discussed in detail.

1 Introduction

While most bearings in industrial applications rotate, there are some notable ones which are required to oscillate. These include bearings in helicopter rotor blade hinges (Tawresey and Shugarts, W. W., Jr., 1964; Rumbarger and Jones, 1968), cardan joints (Breslau and Schlecht, 2020), offshore cranes (Wöll et al., 2018), and blade and yaw bearings in wind turbines, shown in Fig. 1. Blade bearings turn ("pitch") the blade around its longitudinal axis to change the wind's angle of attack as it acts on the blade. Movements in modern turbines mostly consist of small oscillations with the occasional 90 degree movement to bring the turbine to a halt. Similarly, yaw bearings rotate the turbine to face into the wind. Their movements are typically fewer and, depending on the site and the yaw system design, longer.

Rolling bearings under oscillatory movements are commonly associated with wear damage to the raceways and rolling bodies (Behnke and Schleich, 2022; Stammler, 2020; Grebe, 2017; FVA, 2022; de La Presilla et al., 2023). In some cases, such as large amplitudes, varying amplitudes, or the use of oil lubrication, wear is unlikely to occur and rolling contact fatigue becomes more relevant. Engineers should consider both types of damage as a possible failure mechanism and ensure they do not cause a failure of the bearing. This paper reviews calculation approaches to determining the rolling contact fatigue life of oscillating bearings. There are a number of approaches for rolling contact fatigue life calculation in the literature, see Sadeghi et al. (2009) and Tallian (1992) for an overview, but they are mostly intended for rotating applications. While any of these could in principle be changed to be used in oscillating applications, this paper collates all approaches that have explicitly been developed for oscillating bearings in general, or that are concerned with specific bearings which oscillate, such as pitch bearings.

Figure 1. Wind turbine pitch bearing (green, also called blade bearing) and yaw bearing (blue). ©Fraunhofer IWES/Jens Meier

25 An overview of calculation approaches is shown in Section 2. It includes three different commonly used ISO-based factors (Harris, Rumbarger, and Houpert), all of which have been designed for oscillations with a constant amplitude, and a number of other approaches described in the literature. Section 3 gives an overview of experimental results and Section 4 then discusses when to apply these methods, with an example explaining their applicability to pitch and yaw bearings, which oscillate with a varying amplitude.

2 Existing calculation approaches

30 There are a number of publications on the issue of rolling contact fatigue in oscillating bearings. Most of them are based on ISO (ISO, d, c, a, b) or closely related to the model used for ISO. These publications are summarized in Sec. 2.1. Several approaches that have little relation to ISO and its foundations have also been proposed, and are discussed in Sec. 2.2. Some of the ISO-related methods are intended for constant oscillation amplitudes as depicted red in Fig. 2, while some other ISO-related
35 methods and all non-ISO related methods are intended for arbitrary movement as depicted blue in Fig. 2.

2.1 ISO-related approaches

Fundamentally, rolling contact fatigue in oscillating applications is caused by a rolling element repeatedly rolling over locations on a raceway, as is the case in rotating applications. For this reason, many researchers have sought to adapt the well-known ISO approach for rolling contact fatigue calculation to oscillating applications. All of these approaches are hence characterized

40   by the fact that they are based on Lundberg and Palmgren (1947), who proposed that

$$\ln\frac{1}{S} \sim \frac{\tau_0^c N^e}{z_0^h} V, \tag{1}$$

where S is the survival probability, τ_0 is the maximum orthogonal shear stress and z_0 its depth under the raceway surface at which τ_0 occurs, N is the number of load cycles (rollovers), and V is the loaded volume.

Lundberg and Palmgren used Eq. 1 to derive their well-known life equation $L_{10,\mathrm{rev}} = (C/P)^p$, with dynamic load rating C

45   and dynamic equivalent load P, which remains the basis for ISO 281 (ISO, d) and ISO/TS 16281 (ISO, c) as well as countless other publications. They assumed the bearings to be rotating. $L_{10,rev}$ then gives the number of millions of revolutions at which 10% of bearings are expected to suffer the first visible raceway damage[1]. In principle, their derivation can be adapted for use in oscillating movement as well. This section discusses publications which either apply or derive such adaptations of the original Lundberg-Palmgren approach, or approaches very similar to it but also based on Eq. 1. Most of these approaches derive

50   corrective factors a_{osc} that are intended to be applied to a life measured in revolutions and convert it into a life measured in oscillations, i.e.,

$$L_{10,\mathrm{osc}} = a_{\mathrm{osc}} L_{10,\mathrm{rev}}, \tag{2}$$

where $L_{10,osc}$ is the life measured in oscillations and $L_{10,\mathrm{rev}}$ is the life in revolutions. This equation applies to all so-called "oscillation factors" in this paper. For small oscillation amplitudes, a_{osc} typically becomes very large.

55   There are two possible definitions of an oscillation "amplitude"; this paper mainly uses θ as defined in Fig. 3. Some equations are also given in terms of the double amplitude φ if there are differences to the equation in terms of θ. For small oscillation amplitudes, much of the existing literature will predict a high likelihood of wear, particularly for grease-lubricated bearings (Behnke and Schleich, 2022; Stammler, 2020; Grebe, 2017; FVA, 2022). Nonetheless, as discussed in Sec. 3 of this review, it is definitely possible for rolling contact fatigue to occur without wear[2] even for oscillating amplitudes as low as $\theta = 1°$ ($\varphi = 2°$).

60   ### 2.1.1   Harris: Traveled distance

The Harris factor[3] is given in various editions of *Rolling Bearing Analysis* by Harris (Harris, 2001; Harris and Kotzalas, 2007). It considers the effect whereby an oscillating bearing will, depending on the oscillation amplitude, experience a different number of stress cycles on the rings than a rotating bearing. The factor can be interpreted as a conversion of traveled distance into an equivalent number of rotations. For the angle definition in Fig. 3, the total traveled arc A during one oscillation amounts

65   to $A = 4\theta \,(= 2\varphi)$. The Harris factor is then simply

$$a_{\mathrm{Harris}} = \frac{360°}{A} = \frac{90°}{\theta} \left(= \frac{180°}{\varphi} \right). \tag{3}$$

---

[1]Or rolling element damage as per ISO 281(ISO, d); strictly speaking this is not included in the derivation by Lundberg and Palmgren (1947) but ISO included it in the definition of life, presumably because it rarely occurs anyway.

[2]The references for which this statement applies use oil lubrication.

[3]This approach has also been referred to as "Harris 1" in some publications (Schwack et al., 2016; Schmelter, 2011; FVA, 2021; Wöll et al., 2018) to distinguish it from the Rumbarger effect (cf. Sec. 2.1.2), which they falsely attribute to Harris, thus denoting it "Harris 2".
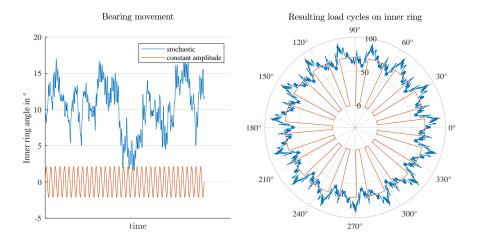
Figure 2. Load cycles resulting from oscillation and stochastic movement in a bearing with $Z = 15$ rolling elements.

Thus, taking an exemplary bearing that oscillates with an amplitude of $\theta = 10°$ and that, if it were rotating, would have a life of $L_{10,\text{rev}} = 1$ million revolutions, and applying Eq. 2 and Eq. 3 gives a life of $L_{10,\text{osc}} = \frac{90°}{10°} L_{10,\text{rev}} = 9$ million oscillations according to the Harris factor. This is because it will execute an arc of $A = 40°$ per oscillation, which is considered as $1/9^{\text{th}}$

70   of a rotation by the Harris factor.

Several references (e.g., IEC (2019)) recommend the use of a so-called load revolution distribution (LRD) or load duration distribution (LDD) for rotating bearings. LRDs sum the number of revolutions at a given load. It is possible to use this approach for oscillating bearings, too, if oscillations are summed and equated to one revolution for every $360°$ of movement. Doing so is in principle identical to using the Harris factor. For a constant rotational speed, LDDs are identical to LRDs; for varying speeds

75   they are merely an approximation.

The Harris factor can be seen as a simplification that neglects two separate effects which may occur in oscillating bearings as opposed to rolling ones. It does not take account of the fact that the load distribution on the moving ring over time is different in an oscillating bearing, a fact originally taken into account by Houpert (1999), nor that only part of the raceway may

80   be loaded[4], originally described by Rumbarger and Jones (1968). A combination and correction of some of the errors in the two aforementioned approaches has been proposed by Breslau and Schlecht (2020) as well as by Houpert and Menck (2021). These approaches are discussed in the following sections.

---

[4]More generally: that there may be a difference in the number of stress cycles for different circumferential locations of the rings, as shown in Fig 2, right. However, Rumbarger only considered differences caused by the fact that some parts of the raceway are unloaded in his publications.
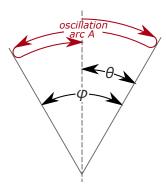
Figure 3. One oscillation covering arc $A = 4\theta\ (= 2\varphi)$ with oscillation amplitude θ (and double amplitude φ) as defined in this paper.

2.1.2 Rumbarger: Partially loaded volume

The Rumbarger effect[5] was originally introduced by Rumbarger and Jones (1968) as early as 1968. This original publication,
which has been described as "complex and impracticable" (Breslau and Schlecht, 2020), was then simplified in Rumbarger
(2003) and NREL DG03 (Harris et al., 2009), but without a derivation of the approach[6]. Each of these publications introduces
an adjusted load rating[7] C_{osc} for oscillating bearings, and using this in $L_{\mathrm{osc}} = (C_{\mathrm{osc}}/P)^p$ gives the life in oscillations. It
is possible to introduce an oscillation factor[8] a_{osc} that produces identical results to the adjusted load rating C_{osc}, cf. App. A
or Wöll et al. (2018). In Appendix A of this paper, the authors include a derivation of the simplified approach and in Appendix B
a discussion of inaccuracies and assumptions contained therein.

Aside from the effects also considered by Harris, the Rumbarger effect is based on the assumption that for small oscillation
amplitudes, only a part of the raceway may ever be loaded. The loaded volume V of Eq. 1 and its load cycles N are then
adjusted accordingly, depending on the given oscillation amplitude[9]. Rumbarger does so by defining the angle θ_{crit} (φ_{crit}) as

$$\theta_{\mathrm{crit}} = \frac{360°}{Z\,(1\pm\gamma)}, \left(\varphi_{\mathrm{crit}} = \frac{720°}{Z\,(1\pm\gamma)},\right) \tag{4}$$

---

[5]This approach has also been referred to as "Harris 2" in some publications (Schwack et al., 2016; Schmelter, 2011; FVA, 2021; Wöll et al., 2018) due
to Harris' authorship of the NREL DG03 (Harris et al., 2009). Since the earliest publications of this approach in the literature are by Rumbarger, and since
Rumbarger was a co-author of NREL DG03, he is credited with the idea here.

[6]Breslau and Schlecht (2020) give a more appropriate treatment of this effect by introducing the factor $a_{\mathrm{osc},2}$ with their Eq. 19. This was further simplified
by Houpert and Menck (2021) into a corrective factor called $f_{\theta\_\mathrm{crit\_i,o}}$ in their Eq. 45, here used for the recommended approach. Although Rumbarger uses
an adjusted load rating while the other authors use corrective factors, all of these approaches attempt to consider the same effect. The differences arise only
because of simplifications in Rumbarger's derivation, cf. Appendices A and B.

[7]Called C_{osc} in Rumbarger and Jones (1968), C_{ao} and C_{ro} for axial and radial bearings in Rumbarger (2003), and $C_{a,osc}$ in Harris et al. (2009).

[8]Called a_{prt} in App. A and $a_{osc_n Ha2}$ in Wöll et al. (2018).

[9]The Harris factor, cf. Eq. 3, does not consider that only part of the raceway is loaded for small oscillation angles. Since it merely adjusts the standard
(rotation-based) calculation approach by the effect of the difference in traveled distance, it implicitly assumes the same loaded volume as in a rotating bearing.

95 where the minus $(-)$ sign refers to the outer raceway and the plus $(+)$ one to the inner raceway, and γ is a common auxiliary factor used in rolling bearing calculations related to the geometry of the bearing[10]. θ_{crit} is the oscillation amplitude required to move a rolling element from its initial location on a raceway to that of the next rolling element. Figure 4 shows stressed volumes above and below the critical angle on an inner raceway. The Rumbarger factor as recommended by the authors of this paper is given by[11] (see Tab. A1 for e)

100
$$a_{\mathrm{Rumbarger}} = \begin{cases} \left(\frac{\theta}{\theta_{\mathrm{crit}}}\right)^{1-1/e} \cdot a_{\mathrm{Harris}} & \text{for } \theta < \theta_{\mathrm{crit}}, \\ a_{\mathrm{Harris}} & \text{for } \theta \geq \theta_{\mathrm{crit}}. \end{cases} \tag{5}$$

For $\theta < \theta_{\mathrm{crit}}$, only part of the raceway volume is loaded during operation. For this case, Rumbarger (2003) and Harris et al. (2009) give a load rating that is derived in Appendix A. This derivation makes some simplifications, and Appendix B shows the errors that occur when using Rumbarger's derivation. If applied correctly, the factor (or load rating) should shorten the life of a bearing as compared to Harris[12], though the simplified factor (or load rating) sometimes increases the life for no other

105 reason than the simplifications made in its derivation. The recommendation in Eq. 5 is thus based on Appendix A without any simplifications. Note that, since θ_{crit} differs between the inner and outer races, so does $a_{\mathrm{Rumbarger}}$. Amplitude θ_{crit} of the outer raceway may be used if a more conservative estimate for the entire bearing is desired[13].

For values of $\theta \geq \theta_{\mathrm{crit}}$, the simplified approach published in Rumbarger (2003) and Harris et al. (2009) is identical to using the Harris factor. This, too, is merely an approximation: Strictly speaking, the life of an unevenly stressed volume (as illustrated

110 in Fig. 4, yellow and blue) is not the same as that of an evenly stressed volume which occurs in a rotating bearing (identical to Fig. 4, red). Appendix C proposes an extension of the Rumbarger factor for such situations, but also concludes that the difference in the factor as compared to a_{Harris} is almost negligible in most cases. The recommendation in Eq. 5 thus follows the above-mentioned publications.

The Rumbarger effect does not consider the effects of an uneven load zone on the moving ring, which are covered by

115 Houpert. Moreover, it assumes that no slippage of the rolling element set occurs, which would move load cycles to occur on different positions of the ring circumference. For a properly installed bearing, Rumbarger and Jones (1968) demonstrated that this assumption can hold true.

---

[10]It is defined as $\gamma = \frac{D\cos\alpha}{d_{\mathrm{m}}}$, where D refers to the rolling body (ball or roller) diameter; d_{m} gives the so-called pitch diameter, i.e., the mean of the inner and outer raceway diameters; and α is the contact angle, where $\alpha = 0°$ is a purely radial bearing and $\alpha = 90°$ is a purely axial one.

[11]Eq. 5 is identical in terms of φ.

[12]In contrast to the Harris effect, with the Rumbarger effect two competing effects ultimately cause a reduction in life. The loaded volume is lower, which increases life; but the load cycles on that small volume which is loaded are higher, thereby decreasing life. The second effect is stronger and reduces the overall life of the bearing, cf. Eq. A3.

[13]Since the traveled distance of a rolling element contact in the rolling direction x is identical on the inner and outer raceways, but the outer raceway's circumference is longer than the inner raceway's circumference for contact angles $\alpha \neq 90°$, the Rumbarger effect is relatively more detrimental to the outer race: It creates a larger deviation from the loaded volume of a rotating bearing than on the inner ring.
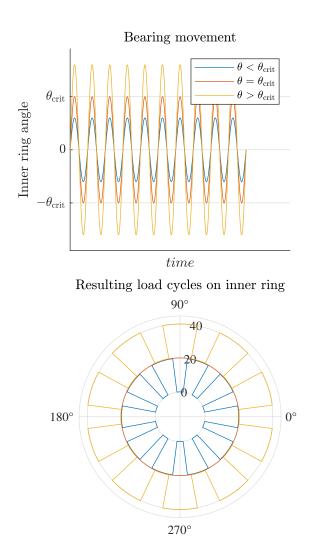
Figure 4. Rumbarger effect: stressed volume as a function of θ relative to $\theta_{crit,i}$ in a bearing with $Z = 10$ rolling elements and a stationary outer ring. Part of the volume experiences zero stress cycles for $\theta < \theta_{\mathrm{crit}}$. For $\theta \geq \theta_{\mathrm{crit}}$, the entire volume is stressed.

2.1.3 Houpert: Load zone effects on the moving ring

The Houpert effect was originally covered by Houpert (1999), with a small error in its derivation. This was corrected by Breslau and Schlecht (2020) as well as Houpert and Menck (2021)[14]. Aside from the effects also considered by Harris, the Houpert

---

[14]Breslau and Schlecht (2020) employ a thorough calculation of the effect only for oscillation amplitudes $\theta > \theta_{\mathrm{crit}}$, cf. Section 2.1.2. For a circumferentially loaded ring with oscillating motion, they thus introduce the load integrals called $J_{\theta a,\psi}$ and $J_{\theta a}$ in their Eqs. 32 and 33. Houpert and Menck (2021) derive an equivalent load called $Q_{\mathrm{eq}}(\psi)$ in their Eq. 35. This term differs from that derived by Breslau and Schlecht (2020) because they (Breslau and Schlecht) use a calculation approach resembling that of Lundberg and Palmgren (1947) and ISO (d), whereas Houpert and Menck (2021) use an approach close to that used by Dominik (1984). The approach used by Dominik is very similar to that of Lundberg and Palmgren, but uses different sets of equations. These two

effect considers that the stress cycle history of the moving ring will be different for an oscillating bearing than for a rotating one.

In the standard life calculation as pioneered by Lundberg and Palmgren (1947) or used in ISO 281 (ISO, d), the load zone is assumed to be constant relative to one ring (called the stationary ring, typically the outer ring). From the viewpoint of

125 Houpert's considerations, movement of the other ring (rotating or oscillating, typically the inner ring) then does not change the load distribution of the stationary ring's raceway. This ring is loaded identically for rotating or oscillating operation. Thus, a_{Harris} gives the correct life of the stationary ring according to Houpert's derivation.

For the moving ring, however, the Houpert effect predicts a different value to a_{Harris}. Since Harris merely adjusts the standard (rotation-based) calculation approach by the effect of the difference in traveled distance, he implicitly assumes that

130 the effect of the load zone is the same as that in a rotating bearing[15]. Thus, a_{Harris} implicitly assumes an element as depicted in blue in Fig. 5 moves through the entire load zone once for each $360°$ of movement[16]. However, in reality this only applies for oscillations where $\theta = i \cdot 180°$ ($\varphi = i \cdot 360°$), $i = 1, 2, 3...$, because for these values of θ each element will move around the entire raceway $2 \cdot \theta = i \cdot 360$ times per oscillation ($\varphi = i \cdot 360$ times per oscillation). For very small oscillations $\theta \to 0°$ ($\varphi \to 0°$) on the other hand, the elements increasingly converge toward the stress cycle history seen in a stationary ring, see

135 Fig. 5. The Houpert factor is generally at or in between the following extreme cases

$$
a_{\mathrm{Houpert}} = \begin{cases} a_{\mathrm{Harris}} & \text{for } \theta = i \cdot 180 \text{ with } i = 1, 2, 3, \ldots \\ & \text{or: purely axial load } (\varepsilon \to \infty) \\ a_{\mathrm{Harris}} \text{ with both rings} & \text{for } \theta \to 0. \\ \text{stationary relative to load} & \end{cases} \tag{6}
$$

In between these extreme cases, detailed calculations have to be performed, curve fits of which can be found in Houpert and Menck (2021). They depend on a value ε, a measure of the load zone size[17]. If applied correctly, the Houpert factor will either be identical to a_{Harris} in the above given cases or shorten the life of the bearing in all other cases. The Houpert effect is thus

140 most noticeable for narrow load zones and small oscillation angles. Houpert and Menck (2021) find deviations which differ by up to 22% from those given by the Harris factor for very narrow load zones and small oscillation amplitudes using ISO exponents (cf. Table A1) and larger deviations of up to 52% using exponents given by Dominik (1984). This is due to Dominik using a higher Weibull slope of $e = 1.5$. Houpert and Menck (2021) give curve fits to calculate the Houpert factor[18] for ball

---

approaches ultimately give almost identical results if similar empirical exponents (cf. Table A1) are used, but details differ, hence the derivation by Houpert and Menck (2021) includes a term called H that cancels out whereas that by Breslau and Schlecht (2020) does not.

[15] As does Rumbarger, who uses the same equivalent load for an oscillating ring as for a rotating one in Rumbarger and Jones (1968), and also in Rumbarger (2003), cf. App. A.
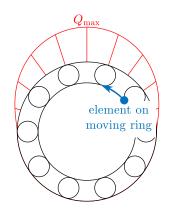
[16] $360°$ of movement consisting, for example, of 9 oscillations with $\theta = 10°$.

[17] Common formulae for ε in the literature tend to be based on small bearings where the rings can be assumed to be stiff. For bearings with large deflection of the rings, based on e.g., FE simulations, different formulae for ε must be used to approximate it, see Houpert and Menck (2021). For multi-row bearings, each row's ε must be determined independently. Either the life of each row is then calculated independently and combined into a total bearing life, or the lowest ε value is taken as a conservative measure.

[18] The reference calls the Houpert factor $a_{\mathrm{osc}\_...}$, and includes in it a corrective factor for the Rumbarger effect, denoted f_{θ_crit}. If only the Houpert factor is desired, $f_{\theta\_crit} = 1$ can be used for the equations in the reference.

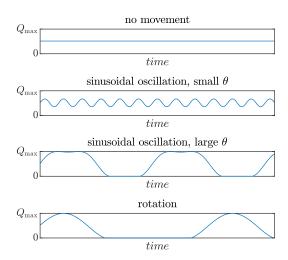**Figure 5.** Houpert effect: load history of an exemplary element as a function of movement relative to load zone. Small θ are similar to no movement, large θ are similar to rotation.

and roller bearings. If ISO/TS 16281 (ISO, c) is used for the life calculation, the extreme case of small theta ($\theta \rightarrow 0$) can be

145   taken into account by assuming both rings are stationary relative to the load and using a_{Harris}.

Strictly speaking, the Houpert effect is not independent of the Rumbarger effect, but for its derivations in Breslau and Schlecht (2020) and Houpert and Menck (2021) it is assumed to be.

2.1.4   Other ISO-related approaches and further literature

The above three factors have been covered in a number of publications, and Breslau and Schlecht (2020) as well as Houpert

150   and Menck (2021) present the most up-to-date models which include them. Besides the above given publications, there are a

number of additional approaches and applications of the above methods. Since all of the above cases are intended for constant oscillation amplitudes, some alternative approaches have been developed which are also intended to be usable for stochastic movement, which leads to different load cycles[19] on the bearing rings as depicted in Fig. 2, blue.

Menck (2023) generalized the Lundberg-Palmgren method to a discrete model ("The Finite Segment Method") that can be applied to arbitrary movement. The model applies Eq. 1 to segments of a bearing. The movement of the balls relative to the inner and outer rings for each discrete simulation point are analyzed for potential stress cycles on the respective rings. For each stress cycle N, the variables τ_0, z_0, and V in Eq. 1 are then directly evaluated and the corresponding damage according to the Palmgren-Miner hypothesis is calculated. The individual survival probabilities of all segments can then be combined into a total bearing life. The model thus encompasses previous use cases and includes the Rumbarger and Houpert effect, but can also be used for arbitrary movement and load histories. Menck (2023) shows the model to produce effectively identical results to ISO 281 for simple use cases which are defined by assumptions identical to those of Lundberg and Palmgren (1947), and reproduces results of oscillating bearings from Houpert and Menck (2021), but also applies the model to a rotor blade bearing of a wind turbine.

Wöll et al. (2018) present a "numerical approach" to calculate the life of a bearing subjected to arbitrary time series. Their model evaluates the life of the whole[20] bearing at every discrete time step of the simulation and then calculates the inferred damage according to Palmgren-Miner for every time step, based on the movement that occurred[21]. The model is shown to be identical to a bin count using the Harris factor, cf. Sec. 2.1.1, for simple sinusoidal movements. For a stochastic time series, their numerical approach produces a shorter life than either Harris'[22], Rumbarger's[23], or Houpert's approaches applied to a bin count. Because Wöll et al. (2018) published in 2018, they still use the erroneous Houpert factor from 1999 rather than more recent results, cf. Sec. 2.1.3, hence they obtain a longer life with the Houpert factor even though there is no physical reason for such an increase. Furthermore, they compare a bin count using the approaches of Harris, Rumbarger, and Houpert and obtain results that are higher than those of the numerical approach with all three bin count approaches including Harris, and conclude that using these bin counts "overestimates the lifetime for non-sinusoidal loads and speeds". They also produce a simple method to calculate an equivalent load for oscillating loads but it fails to take local effects into account as accurately as Menck (2023).

Schwack et al. (2016) do not present a new model but compare factors from Harris, Houpert, and Rumbarger. They also include an approach denoted "ISO", which is identical to that of Harris. Having published in 2016, the authors also use the erroneous model of Houpert (1999) that was later corrected (cf. Sec. 2.1.3). Moreover, their application of the Houpert

---

[19]The term "load cycles" is used here synonymously with "rollovers". Load cycles in Fig. 2 were determined by using the inner ring angle θ_i as depicted on the left-hand side of Fig. 2 (outer ring assumed stationary) to calculate the movement of the cage $\theta_c = 0.5 \cdot \theta_i \cdot (1 - \gamma)$. This was then used to obtain relative cage movement on the inner ring $\theta_{rel,i} = \theta_i - \theta_c$. A change in $\theta_{rel,i}$ is then considered a load cycle on the respective position where it occurred.

[20]The fact that Wöll et al. use the *whole* bearing life is the critical difference to Menck's Finite Segment Method, cf. Menck (2023), Sec. 2.2.

[21]One may evaluate the life and the corresponding movement of the bearing as shown in Sec. 2.1.6 with each time step used as a bin, and using only the Harris factor. This is identical to their numerical approach.

[22]Called "Harris 1" in the reference.

[23]Called "Harris 2" in the reference.

factor is not recommended for double-row bearings with large structural deformation[24]. Their evaluation of the Rumbarger factor[25] results in a longer life than using the Harris factor[26]. As explained in Sec. 2.1.2, this increase only occurs because of simplifications in the derivations performed by Rumbarger but for no physical reason, since the effects considered should shorten the life, not prolong it. The relatively large deviations from a_{Harris} shown in Schwack et al. (2016) are therefore both due to inaccuracies in the factors that were used.

Hai et al. (2012) propose a generalization of ISO 281 specifically for slewing bearings. They divide the bearing into several segments in a similar way to Menck (2023), but unlike Menck's, their segment width depends directly on the oscillation amplitude. They also make a number of simplifications not made by ISO 281 or Menck[27]. Their model can be used for individual operating conditions with either rotation or a constant oscillation amplitude; however, several conditions with different amplitudes may also be combined using equivalent loads and equivalent oscillation amplitudes for the segments. They compare their results to an exemplary calculation of NREL DG03 and conclude that their somewhat similar results validate the method. The simplifications made make it difficult to establish whether their method is actually more accurate than simply using the oscillation factors given above.

2.1.5 Further effects during oscillation

Further effects occur during oscillation which are not considered by any of the above approaches.

When a rolling element passes completely over a position on the raceway, the orthogonal shear stress below the surface changes from maximum $(+\tau_0)$ to minimum $(-\tau_0)$. This is the typical stress cycle assumed in all ISO-based approaches mentioned here; it is depicted in Fig. 6 on the left. This load cycle does not take place to the full extent at the outer ends of an oscillation cycle as depicted in Fig. 3. For raceway positions close to the reversal points of the oscillation, the direction of the load cycles changes; this phenomenon is depicted in Fig. 6 (oscillation, red case). The shear stress of the volume close to the reversal points does not fully span from $+\tau_0$ to $-\tau_0$ but is stopped prematurely; this too is depicted in Fig. 6 (oscillation, blue case). Similarly, for oscillations with small amplitudes, the stress range does not extend to the maximum and minimum of a passing contact in rotation, see Fig. 6 (small oscillation). None of these effects is considered in the ISO-based approaches named herein.

---

[24]The publication in question uses a single ε value for a large four-point slewing bearing that is based on deformations in Finite Element (FE) simulations. The purpose of ε in Houpert's approach lies in its ability to describe the load zone of a race. Thus, each inner-outer raceway pair should get an ε value for a proper calculation, as each of them may have a different load zone. Moreover, determining ε based on deformations that occur in FE simulations can be misleading for large slewing bearings, since they tend to have a lot of structural deformation, but common equations given for ε are mostly based on assumptions of rigid races. Various suggestions for the derivation of ε, including ones for large slewing bearings, can be found in (Houpert and Menck, 2021).

[25]Called "Harris 2" in the reference.

[26]Called "Harris 1" in the reference.

[27]Because their approach is intended for slewing bearings, they assume the contact ellipse dimensions a and b as well as z_0 to be identical on the inner and outer rings; they approximate $z_0 \approx 0.5b$ and $\tau_0 \approx 0.25 P_{\mathrm{max}}$, which is only completely correct for roller bearings but not ball bearings; they assume the cage moves at half the speed of the rotating ring, which is only true if a purely axial contact of $\alpha = 90°$ is present; and they assume the critical angle to be identical for the inner and outer rings, using $\theta_{\mathrm{crit}} = 360°/Z$ for both rings.
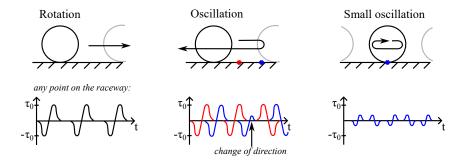
Figure 6. Left: load cycle as assumed by all ISO-based approaches; other examples: further types of load cycles not considered in ISO.

The thickness of the lubricant film is affected by oscillation, and may even become so poor that wear rather than fatigue becomes the dominant damage mechanism. Numerous studies investigate wear phenomena in oscillating bearings; for a review,
205 see de La Presilla et al. (2023). As far as the authors are aware, there are no simple models to estimate the thickness of the lubrication film as a function of the oscillation and thus determine its potential effects on rolling contact fatigue. Such an estimation would likely become even more challenging with grease lubrication due to the effect of the thickener. Therefore, the effect of lubrication is mostly ignored in all models of which the authors are aware. This statement also applies for the non-ISO based approaches discussed in Sec. 2.2.

210 **2.1.6 Binning**

Life calculations often need to be performed for operating conditions that vary over time. The most accurate way to calculate the rolling contact fatigue life of a bearing under varying operating conditions according to the assumptions in Eq. 1 made by ISO-related approaches is to use the Finite Segment Method according to Menck (2023), because it considers local load changes rather than summing global, location-independent bearing damage over time. For most users, it will however be simpler to
215 remain closer to existing approaches that are based on C and P and do not require a more detailed calculation approach with local damage calculation. Doing so for oscillating bearings necessitates the use of bins in combination with oscillation factors (Harris, Houpert, or Rumbarger). This is the most commonly recommended approach, a version of which is also found e.g., in the NREL DG03 (Harris et al., 2009). Using bins is merely an approximation, since the aforementioned factors have all been developed for constant oscillation amplitudes around the same mean position and they all assume there is a constant load
220 acting on the bearing as it moves, along with a number of other assumptions made by Lundberg and Palmgren (1947).

To apply oscillation factors, movement such as depicted in the stochastical case of Fig. 2 must be translated into bins of oscillations. Typically, variable load is taken into account in fatigue calculations by using rainflow counting (ASTM, 2017). Rainflow counting is also used for the bearing movement (as opposed to the load) for the life calculation of pitch bearings in

NREL DG03[28], Menck et al. (2020), and Keller and Guo (2022).[29] Performing a rainflow count will provide the bins required for further calculations.

The load acting on the bearing is irregular and must be simplified into a single equivalent load P for each bin of the cycle count. Ideally, to this end, the equivalent load P per time step is determined and the equivalent load over the bin is determined from all time steps $i = 1...n$ in the bin as per

$$P_{\mathrm{m}} = \left(\frac{N_1 P_1^p + N_2 P_2^p + \ldots + N_n P_n^p}{N_1 + N_2 + \ldots + N_n} \right)^{1/p} . \tag{7}$$

This approach is not specific to oscillation and can similarly be found in various bearing manufacturer catalogs and basic machine element text books (Schaeffler Technologies AG & Co. KG, 2019; Liebherr-Components AG, 2017; Roloff et al., 1987; Decker, 1995; Haberhauer and Bodenstein, 2001). The value $N_i = n_i \cdot \Delta t_i$ here represents the distance covered in the condition i (measured in degrees or revolutions), and can be calculated from the speed n_i and the time t_i in that condition[30]. The exponent p is given in Table A1.

If it is not possible to determine P_{i} for each time step, potentially due to the calculation being too costly, it is possible to apply Eq. 7 to the force and moment components making up P (including radial force F_{r}, axial force F_{a}, and bending moment M) and to then determine $P_{\mathrm{m}} = f(F_{\mathrm{r,m}}, F_{\mathrm{a,m}}, M_{\mathrm{m}})$ from their values for each bin (calculated as per Eq. 7, but using $F_{\mathrm{r}}, F_{\mathrm{a}}, M$ instead of P).

Using the P_{m}-values of each bin, it is now possible to calculate the life of each bin $L_{\mathrm{rev}} = (C/P_{\mathrm{m}})^p$. The life in oscillations L_{osc} according to Eq. 2, using the appropriate factor as determined on the basis of Sec. 4, can be determined too.

All of the bins $b = 1...B$ obtained are then typically combined into one final life using the Palmgren-Miner hypothesis according to

$$L = \frac{\phi_1 + \phi_2 + \ldots + \phi_B}{\frac{\phi_1}{L_1} + \frac{\phi_2}{L_2} + \ldots + \frac{\phi}{L_B}}, \tag{8}$$

where $L_1, \ldots, L_B$ denotes the life in bin b. This may be either the life in oscillations, revolutions, or time. Typically, the life would be in oscillations if oscillation factors have been used but it may be converted to time or revolutions. The variable ϕ then gives the oscillations, revolutions, or time performed in that bin, but must have the same unit as the life. L denotes the total, combined life of all operating conditions.

It is worth noting that binning is solely used to reduce the number of data points from real-life data or a simulation. Using modern computers, if there is no hardware-specific necessity to reduce the number of data points, the most accurate approach

---

[28]Misspelled as "rainbow cycle" in the reference.

[29]For damage mechanisms like wear, where the order of movement is important, Stammler et al. (2018) recommend range-pair counting. In fatigue calculations, rainflow counting is more useful because it can fully represent the effect of a large movement (or load cycle) that is interrupted by many small ones. However, this effect is only noticeable in rolling contact fatigue calculations if the Houpert effect is considered. Otherwise a range-pair count will produce a very similar result to a rainflow count. This is because oscillation cycles of the moving ring in rolling contact fatigue are different from a load cycle: The load cycles are caused by the rolling elements rolling over the raceway and are thus very local phenomena that are seldom interrupted.

[30]Strictly speaking, this equation only applies for a constant load direction, but it can be used as an approximation with some variations in the load direction, too, as proposed here. The same applies for Eq. 8.

250   is to use each single step taken from e.g., an aeroelastic wind turbine simulation or some other data set and treat it as a separate bin to which Eq. 8 is directly applied, rather than processing the steps into a reduced number of bins. This is both easier and less error-prone, as well as more accurate than binning beforehand. In order to account for oscillation effects, it would then be required to consider the larger oscillation cycle (amplitude) that a specific step is part of and adjust its life based on that, where the step will typically make up a fraction of the complete oscillation.

2.2   Non-ISO related approaches

255   A number of alternative approaches have been developed in recent years, particularly with a focus on blade bearings. Many of these approaches rely on S-N curves that can be determined without testing a complete bearing.

Leupold et al. (2021) segment a bearing and use a reduced Finite Element model in a multibody simulation to determine the stress on each segment. Using bearing movement from time series they obtain the number and magnitude of stress cycles

260   for each segment. Individual loads are combined using the Palmgren-Miner hypothesis. Unlike almost all literature on rolling contact fatigue, their model is based on Hertzian normal contact pressure rather than subsurface shear stress. However, they note that "fatigue criteria such as Fatemi–Socie or Dang Van could also be applied" in subsequent work. They obtain empirical values used for the Palmgren-Miner hypothesis from a test of a full-sized blade bearing[31] and an assumed slope of the S-N curve from the literature, and further note that "a large number of tests are necessary for reliable results".

265   Lopez et al. (2019) propose a model for a blade bearing that uses the movement of the bearing as a basis and computes the multiaxial stress-state at the subsurface of the raceway. Loads are obtained from FE simulations using blade root loads from multibody simulations. They apply various multiaxial fatigue criteria and compare the results. They find that IPC control strategies significantly increase the damage inflicted on a bearing compared to CPC due to the increased movement. The lives calculated with the different fatigue criteria are also sometimes very different from each other.

270   Escalero et al. (2023) propose a method for the probabilistic prediction of rolling contact fatigue in multiple-row ball bearings subject to arbitrary load and movement histories. They use a three-dimensionally discretized model of the raceway in which each finite element's individual stress cycle history over time is analyzed using a rainflow count. They use orthogonal shear stress as the governing parameter but note other criteria may be included in the future. The failure probability of the individual elements is determined based on S-N curves obtained from rotating bending specimens and by applying scale factors because

275   of size differences between the specimen and the elements, and because of the conversion from normal to shear stress. All individual element failure probabilities are combined using the Weibull weakest link principle. The authors demonstrate their method for a reference case in which a blade bearing was tested.

Hwang and Poll (2022) propose an approach that is then further detailed in Hwang (2023). The approach is based on one circumferential position of the inner bearing ring denoted "small stressed volume" (SSV). The stress-load-history of different

280   layers below the race at the SSV is analyzed in detail based on the behavior of the inner ring and the load distribution of the bearing. Residual stresses are optionally included in the calculation. For all load cycles that occur, the Palmgren-Miner hypothesis is applied to layers at the SSV. The layer with the lowest survival probability is used to calculate the life of the

---

[31]Presumably a bearing of the same type as used for the calculation, though this is not specified in the reference.

bearing. To consider the effect of loaded volume, Hwang proposes a simplified method to estimate the loaded volume in the specimens on which his S-N curves are based, and the loaded volume in the bearing, and to correct the bearing life based on this estimation. The model is applied to rotating and oscillating bearings under constant operating conditions. Hwang (2023) further outlines a proposed application of his model to rotor blade bearings that is not carried out in detail.

3   Experimental validation

Despite the large number of theoretical models discussed above, there are only a few published experimental results of fatigue tests on oscillating bearings.

Tawresey and Shugarts, W. W., Jr. (1964) tested approximately 750 oil-lubricated bearings under oscillating conditions closely duplicating those encountered in helicopter rotor blade hinges but failed to produce a logical explanation of their results (Rumbarger and Jones, 1968). Rumbarger and Jones (1968) therefore reanalyzed 388 of these bearings comprising 13 test series of identically sized, caged needle-roller bearings and derived a life calculation approach based on the Lundberg-Palmgren theory, cf. Sec. 2.1.2. They conclude that "the theory of Lundberg and Palmgren is [...] favorably compared with the life tests" and derive an experimental load rating C that is shown to be within the bounds defined by the relevant standards at the time (then ASA and AFBMA, today ANSI and ABMA) when adjusted for oscillating motion according to Sec. 2.1.2. Further, they specifically conclude that "the life varied inversely to the fourth power of the radial load", thus giving $p = 4$, which is identical to the load-life exponent of Lundberg and Palmgren (1952) for the case of pure line contact, cf. also Table A1. For the 13 test series, they derive Weibull slopes ranging from $e = 1.13$ to 3.55, with a mean value of $e = 2.04$. This is higher than the value of Lundberg and Palmgren (1952) and ISO 281 ISO (d), cf. Table A1, but they also note that "the wide variation in the values of the Weibull slope are well known", since different bearing tests routinely produce different Weibull slopes, including even the test data of Lundberg and Palmgren (1952) on which the values of ISO are based; and that the higher Weibull slope may be a product of using more modern steels than those used by Lundberg and Palmgren (1952). Despite the tests going as low as an amplitude of $\theta = 1°$ ($\varphi = 2°$), none of the bearings show evidence of fretting corrosion[32], but the failed bearings presented "varying degrees of flaking breakout or spalling which is characteristic of failure in rolling-contact bearings subjected to rotation".

Halmos et al. (FVA, 2021) use oil-lubricated cylindrical roller bearings for fatigue tests. They obtain rolling contact fatigue for oscillation amplitudes as low as $\theta = 1°$ ($\varphi = 2°$) equaling $x/2b = 1$. The final number of fatigue results is too low to compare them against theoretical calculations, but they conclude that "at least for selected amplitudes, the existing calculation approaches [referring to ISO-based approaches] deliver conservative results compared to the experimentally determined lives".

Münzing (2017) tests seven ball screws with $\theta = \theta_{\mathrm{crit}}$. The lubricant is an aviation grease type Aeroshell 33 MS. The test duration is equivalent to the L_{10} of the ball screws. Five out of seven show initial damage on the raceways. As the standard

---

[32]A common value to compare wear tests on different bearings is the $x/2b$ ratio (Schwack, 2020). Using the data given in the reference, the authors determined this test to correspond to $x/2b \approx 5$.

DIN 631 for ball screws defines a minimum size for surface damage to be considered as fatigue damage and this size is not reached, they are assessed as having passed according to the standard.

Escalero et al. (2023) propose an approach discussed in Sec. 2.2. They compare their results to the test of a single blade bearing under axial load but obtain no correlation. The failure onset in the bearing could not be established exactly as failure already had progressed significantly once it was opened.

Hwang (2023) applies his model to rotating cylindrical roller bearings and angular contact ball bearings as well as four-point bearings. He compares his results to tests of 200 radial cylindrical roller bearings (NU 1006, 55 mm outer diameter) and several double-row four-point bearings of 2.4 m diameter. The model deviates from his experimental results by a factor of about 2 to 10, giving a lower estimate than observed in the tests.

4 Use of the approaches

This section contains recommendations for when to use which approach. Section 4.1 contains a number of general recommendations, Sec. 4.2 and 4.3 discuss some simple illustrative examples, and Sec. 4.4 and 4.5 detail possible uses for a pitch and yaw bearing in a wind turbine.

4.1 Recommendations for use

A flowchart of when to use which method, based on the underlying modeled physical principles, is given in Fig. 7. Theoretically, the conditions in the flowchart must hold all the time. Practically, it will be sufficient if they hold most of the time. Dashed arrows represent mathematical approximations. For the ISO-related approaches, recommendations are given according to the underlying physical phenomena considered in the derivations as described in this paper. The recommendations herein may therefore deviate from those given by the respective authors. For the non-ISO related approaches, recommendations generally follow the respective authors since they rely on less widely acknowledged approaches and may therefore be subject to the more individual interpretation of the respective authors. Further comparisons between the approaches are given in Tab. 2.

Generally, the start of the flowchart is given by the "Start" box. If bins are used (cf. Sec. 2.1.6), the "Start bins" box can be used for an approximation. In this case, the condition $\theta \geq \theta_{\mathrm{crit}}$ applies if all circumferential positions of the ring experience some stress cycles over all bins[33].

None of the ISO-related approaches predicts huge deviations from a_{Harris} for regular operating conditions. For a rough estimate, if the desired life is well below that calculated with the Harris approach, it is very likely to pass with the other ISO-related approaches, too. For a more precise calculation, narrow load zones or small oscillation angles below θ_{crit} will produce the largest deviations from the Harris factor.

---

[33]Since the use of bins represents an approximation, there is no more precise wording than "some stress cycles" for this issue. See e.g. Fig. 2, blue, for an example for which $\theta \geq \theta_{\mathrm{crit}}$ even though individual oscillation amplitudes may be below θ_{crit}. Note that the position of the rolling elements w.r.t. the rings is required for this assessment, not the position of the inner ring, θ_{i}. The position of the rolling elements w.r.t. a stationary outer ring is given by $\theta_{\mathrm{c}} = 0.5 \cdot \theta_{\mathrm{i}} \cdot (1 - \gamma)$; the position of the rolling elements w.r.t. a moving inner ring is then given by $\theta_{\mathrm{i}} - \theta_{\mathrm{c}}$.

For the Rumbarger effect, based on Sec. 2.1.2 and App. A, the flowchart recommends combining this effect with the Houpert effect for non-axial loads (i.e., radial and moment loads). This deviates from Rumbarger and Jones (1968), where the Rumbarger effect is used without consideration of the Houpert effect for radial bearings, and Harris et al. (2009), where the Rumbarger effect is used without consideration of the Houpert effect for moment loads, but this recommendation is based on the fact

345 that particularly for these cases which represent relatively small load zones ε, the Houpert effect is to be taken into account[34].

The flowchart considers the "numerical approach" of Wöll et al. (2018) as well as Hai et al. (2012) to be approximations. Although Wöll et al. use the approach for a series of stochastic movements and load directions, they also note "the numerical approach lacks the capability of taking sophisticated distinctions into account, as [Rumbarger][35] does with the critical angle distinction and Houpert does with comparing the oscillation amplitude to the load zone size". The reason their method cannot

350 consider these local effects is due to the global application of the Palmgren-Miner hypothesis, see Menck et al. (2022), Sec. 2.2. Menck's Finite Segment Method can be seen as a more accurate (but more difficult to implement) version of Wöll's numerical approach that considers local effects also seen with Houpert and Rumbarger. Wöll's numerical approach is also effectively identical to a bin count, listed below it in the flowchart. Hai et al. (2012) is listed as an approximation due to the reasons set out in Sec. 2.1.

355 As noted in App. C, the Rumbarger effect actually applies even for oscillation amplitudes $\theta > \theta_{\mathrm{crit}}$, but since its effect is so small at these amplitudes the effect at larger amplitudes is not considered in Fig. 7.

Some approaches are derived in different sources. The authors recommend using the following sources: The Harris factor is given in Sec. 2.1.1. The Houpert factor is best considered according to the model of Breslau and Schlecht (2020) or Houpert and Menck (2021). The latter reference includes curve fits for ease of use. Older references may be erroneous. The Rumbarger

360 effect is best calculated according to Eq. 5 or Breslau and Schlecht (2020) or Houpert and Menck (2021), cf. also Sec. 2.1.2. Older references may be oversimplified. A combination of the Houpert factor and the Rumbarger factor is best performed according to Breslau and Schlecht (2020) and Houpert and Menck (2021). All other approaches in the flowchart are best performed according to the publications of their respective authors.

4.2 Application to a cardan joint bearing

365 An exemplary cardan joint connects two shafts whose axes are inclined to each other. The shafts rotate, causing the cardan joint bearing to oscillate with a constant oscillation amplitude of $\theta = 5°$. The exemplary bearing is a radial bearing with contact angle $\alpha = 0°$. It contains $Z = 15$ balls with a diameter of $D = 10\,\mathrm{mm}$, and has a pitch diameter of $d_{\mathrm{m}} = 60\,\mathrm{mm}$. The critical amplitude according to Eq. 4 is then $\theta_{\mathrm{crit,o}} = 28.8°$ and $\theta_{\mathrm{crit,i}} = 20.6°$ for the outer and inner raceways, respectively. The load zone is made up of a purely radial load that is constant with respect to the outer ring.

---

[34]This may seemingly contradict the conclusions in Sec. 3, which state that Rumbarger and Jones (1968) already find their results to be consistent with standards despite not considering the Houpert effect. For a radial load giving $\varepsilon = 0.5$ and small oscillation amplitudes, Houpert and Menck (2021) predict a life reduction of about 10% which would still put Rumbarger and Jones' results within the range of the standards at the time. This statement therefore does not contradict Rumbarger and Jones' conclusions.
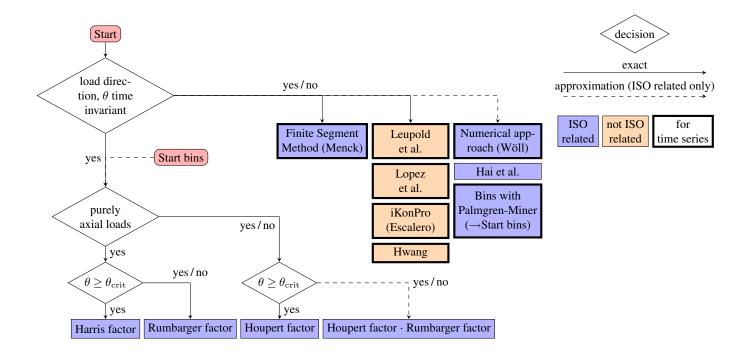
[35]Called "Harris 2" in the reference.

Figure 7. Flowchart to find the simplest applicable life calculation approach for a given oscillating bearing.

Table 1. Comparison of different life calculation approaches

Approach	Based on bearing tests or small specimen S-N curves	Considers partial load cycles (cf. Fig. 6)	Considers volume effect	Considers whole race volume	Stress criterion	Experimental validation
ISO-based	bearing	no	yes	yes	τ_0	ok but incomplete
Leupold et al.	bearing	yes	unclear	yes	normal stress P, pot. more	not available
Lopez et al.	S-N	yes	unclear	yes	various	not available
iKonPro	S-N	yes	yes	yes	τ_0, pot. more	limited data
Hwang	S-N	no	partially	no (only SSV)	various	some deviations

According to Fig. 7, both the load direction and θ are thus time invariant. There is no purely axial load, and $\theta \geq \theta_{\mathrm{crit}}$ does *not* apply. A combination of the Houpert and Rumbarger factors can thus be used by multiplying them as shown in Houpert and Menck (2021), using the Rumbarger factor for the outer race to be conservative. Alternatively, the approach given by Breslau and Schlecht (2020), who discussed cardan joint bearings in their paper in more detail, may be used. Furthermore, the other

approaches in the top right of Fig. 7 may also be used since they apply to general time-series based data and thus also apply to

375 simpler data.

4.3 Application to a crane slewing bearing

An exemplary crane slewing bearing is located at the bottom of a crane which is exclusively used to perform oscillation amplitudes of $\theta = 90°$ to unload a ship. It is an axial bearing with $\alpha = 90°$. The critical amplitude according to Eq. 4 is $\theta_{\mathrm{crit}} = 8°$ for both inner and outer rings. The load is mostly an axial load with only a slight tilting moment component.

380 According to Fig. 7, the load direction is then invariant, and so is the oscillation amplitude θ. The load is (approximately) purely axial, and $\theta > \theta_{\mathrm{crit}}$. Therefore, the Harris factor applies for this bearing.

If θ were time invariant, it would also be possible to use the Harris factor and combine different bins using the generalized mean in Eq. 7. Again, more complicated approaches in the top right of the flowchart would also apply.

4.4 Application to rotor blade bearings

385 A number of publications include rolling contact fatigue calculations for rotor blade bearings, some ISO-related[36], see Harris et al. (2009); Schwack et al. (2016); Menck et al. (2020); Keller and Guo (2022); Menck (2023); Rezaei et al. (2023), and some not, see Escalero et al. (2023); Hwang (2023); Leupold et al. (2021); Lopez et al. (2019). The non-ISO based methods are, as stated in Sec. 4, best applied according to the respective publications given above, though many of these publications are relatively short and likely not sufficient for an end user to actually copy their technique and apply to an actual bearing.

390 Moreover, according to Sec. 3, the experimental validation for these models is still lacking. Therefore this section will focus on ISO-based approaches, which remain the most common life calculation methods for rolling contact fatigue.

Rotor blade bearings typically experience pitch amplitudes as in the stochastic case depicted in Fig. 2: Their oscillation amplitude is irregular, as are the loads acting on the blade in five degrees of freedom. Moreover, the load direction changes slightly, though mostly for smaller loads (Menck et al., 2020). Therefore, according to Fig. 7, the Finite Segment Method (Menck, 2023)

395 would be the most appropriate ISO-based method for an engineer to use. However, some simplified approaches exist, too. These include the methods by Wöll et al. (2018) and Hai et al. (2012), and the approach most often chosen by users, a bin count. Using a bin count is likely the most user-friendly and well-known of the approaches. Section 2.1.6 details how to do a bin count and therefore represents the first step required for calculating the life of a pitch bearing, and this step is described in detail below.

400 At this point we assume bins to be present, where ideally no binning is performed but each time step of the simulation is used as an individual bin (cf. Sec. 2.1.6). Prior to the application of Eq. 8, the lives L_b of each bin must be calculated using an approach which takes the oscillation into consideration. To this end it is useful to refer to Fig. 7. Although both the load direction and pitch angle θ are time invariant, they have to be considered to be approximately constant in order to use oscillation

---

[36]Among the ISO-related publications it is worth noting that NREL DG03 (Harris et al., 2009) is the most common guideline for blade bearing life calculation, and Schwack et al. (2016); Menck et al. (2020); Keller and Guo (2022); Rezaei et al. (2023) are all, at least in part, based on it; only Menck (2023) is not. The publications have not been included in Sec. 2.1 if they merely apply the DG03 but present no new methods or findings relevant to this review.

factors, hence the start at "Start bins". The loads are not purely axial, but the oscillation of the bearing - over the entire operating
time of the turbine - is large enough to have rolling elements cover the entirety of the raceway at one point or another[37]. That is
to say there is no area that is never stressed, giving $\theta > \theta_{\mathrm{crit}}$. The Houpert factor is therefore a useful factor to employ, whereas
the Rumbarger factor is not, since each segment of the raceway will see rolling elements pass by fairly regularly.[38]

Using ISO/TS 16281, there are two different equivalent loads: Q_{ei} for the inner ring and Q_{ee} for the outer ring. For each
of these rings, users must decide whether the ring is rotating or stationary relative to the load. Since rotor blade bearings
mostly perform small oscillations below approximately 20° of amplitude, an alternative to using the Houpert factor is to use
the equivalent load of a stationary ring for both rings in combination with the Harris factor (cf. Sec. 2.1.3). This is equivalent
to the "worst case" scenario of the Houpert factor and is almost identical to it at small oscillation amplitudes.

Figure 8 shows different approaches to calculate the life of a rotor blade bearing using data from aeroelastic simulations.
Table 2 summarizes the approaches. The five approaches are ordered with increasing accuracy to the right of the figure. All
of them are closely related to ISO and therefore to Eq. 1. The first three approaches (name containing "bins") all pre-process
the time series data into bins based on the bearing movement and load data acting in a given time step. The fourth approach
("stepwise") uses each individual time step of the simulation as a separate bin. The fifth method ("Finite Segment Method")
does not use binning but directly calculates damage based on the number of rollovers occurring in segments of the ring. This is
the most accurate method and can be used as a reference for the others. Results for the first four methods have been obtained
using ISO/TS 16281 for the equivalent load. All results are displayed using the Harris factor, if applicable (that is, if bins were
used in some form), assuming one ring to be rotating in ISO/TS 16281; and using a more accurate method for oscillation,
which means that both rings have been calculated as stationary according to ISO/TS 16281 in combination with the Harris
factor. The Finite Segment Method automatically includes effects of oscillation and cannot be used with the Harris factor.

The first three approaches shown in Fig. 8 involve pre-processing into bins. It can be seen that some of their results deviate
more, some deviate less from the Finite Segment Method. These results are heavily dependent on details of the pre-processing
used for the data and the results shown here are not representative for other potential types of pre-processing. The fact that the
"coarse bins"-simulation using an oscillation correction is so close to the Finite Segment Method is thus likely accidental and
not because this particular approach is particularly representative of a more correct method.

Comparing the life $L_{10,\mathrm{stepwise}}$ of the stepwise calculation where one ring is assumed to be stationary and one is assumed to
be rotating ("Harris factor/LRD") to the results $L_{10,FSM}$ of the more accurate Finite Segment Method, one can see that

$$L_{10,\mathrm{FSM}} = 0.86 \cdot L_{10,\mathrm{stepwise}}. \tag{9}$$

This is roughly in line with using the Houpert factor or assuming both rings to be stationary, which gives a result which is
only slightly higher (cf. Fig. 8, stepwise, Oscillation correction). The result of the Finite Segment Method is slightly lower

---

[37]Individual pitch cycles may cover only a small portion of the raceway, but this only causes deviations as large as those given by the Rumbarger factor
if this behavior continues for the bulk duration of operation along the same mean position with the same amplitude, which is not the case in a typical pitch
bearing.

[38]Note that this recommendation is in contrast to the current version of NREL DG03, which uses the Rumbarger effect only (by modifying the load rating -
equivalent to using a factor as discussed in Sec. 2.1.2).

Table 2. Different approaches to calculate the life of a rotor blade bearing

Denomination	Details
coarse bins	1 080 bins with the upper load level per bin used for P
fine bins	151 200 bins with the upper load level per bin used for P (Implementation of Menck et al. (2020))
fine bins, P_{m}	Identical to "fine bins" but using generalized mean loads P_{m} of each bin according to Eq. 7
stepwise	Creates one individual bin per simulation time step
Finite Segment Method	Sums damage from individual rollovers on individual locations of the rings (Implementation of Menck (2023))

because it first sums local damage over the entire span of the simulation before determining the global bearing life. Therefore,

435   load concentrations on individual segments and bearing rings are considered more accurately than with the other methods[39]. For calculations performed with ISO-related approaches using binning of data in some form, where one ring is assumed to be stationary and one is assumed to be rotating[40] it is therefore reasonable to expect a life which is 10 to 15% longer than that obtained with more advanced methods. Further deviations that are caused by binning of the data and other forms of pre-processing are impossible to predict and therefore a stepwise calculation is preferable.

440   **4.5   Application to yaw bearings**

For yaw bearings, the oscillation behavior is highly site dependent. Any wind direction history can be calculated using the Finite Segment Method or the other approaches highlighted with thick borders in Fig. 7. For the design of a wind turbine, yawing movements are seldom simulated, apart from a few design load cases (Wenske, 2022). Rather, constant offsets from an optimal yawing position are simulated and assumed to be present for a certain amount of operating time. Yaw movement

445   is then assumed to be distributed among these simulated cases. The design of yaw bearings thus lends itself to binning, since detailed time series will typically not be available.

---

[39]The result of the Finite Segment Method may thus also by influenced slightly by the Rumbarger effect, i.e., an uneven distribution of rollovers along the circumference, although the effect is much less than would be predicted by the Rumbarger factor if applied directly to the individual pitch cycles. It also captures potential load concentrations on individual raceways because the life of the raceways is determined from their individual segments, therefore including a load history for the raceways too, whereas with the other methods the raceway life is included in a bearing life which is then used for the Palmgren-Miner hypothesis, leading to a loss of information.

[40]This is the standard assumption in virtually all typical rolling contact fatigue life calculations including ISO 281.
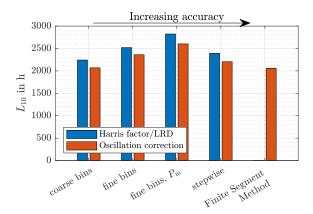
Figure 8. Comparison of the different approaches in Tab. 2 with Harris factor and additional effects for oscillation considered.

Though the behavior is highly dependent on both the site of the turbine as well as the design of the yaw system, some general statements can be made. Firstly, even at sites with only one main wind direction, it is likely that this wind direction will vary by a few degrees. Secondly, the yaw misalignment that triggers a yaw movement is dependent on the yaw system design. Yaw misalignments of $3°$ to $8°$ are common, realistic values (Wenske, 2022). Finally, the design of large scale yaw bearings, like that of pitch bearings, usually includes a large number of rolling elements in excess of 50 or even 100 and more per row, giving small critical angles θ_{crit}. It is thus unlikely that any yaw bearing will be operated in a manner whereby during the entire operating history of the bearing, the loads are truly concentrated only on parts of the raceway, since that would require yaw movements to be consistently smaller than θ_{crit} despite fluctuations in the wind direction and possible slippage of the rolling element set. The Rumbarger effect is thus unlikely to be relevant for yaw bearings in the field.

Regarding the Houpert effect, the wind direction is important. Unlike for typical bearings, the rotating (oscillating) ring is the one that will always be loaded in one primary position since it is consistently moved toward the wind. The stationary ring, on the other hand, can experience very concentrated loads in one position (in the case of a site with only one main wind direction) or it can even experience loads spread evenly over its circumference (on sites with no clear main wind direction, where the wind can come from any direction). In the first case (one main wind direction only), similar to pitch bearings, both rings experience a high concentration of loads in one spot. It is thus recommended that the Houpert effect is considered, ideally by using the equivalent load for a stationary ring, for the calculation of both Q_{ei} and Q_{ee} if ISO/TS 16281 is used. Otherwise, the Houpert effect can be taken into account by using the publications mentioned in Sec. 4.1. Assuming one main wind direction is the more conservative assumption and should be the approach to choose in case of doubt. Since yaw bearings, like pitch bearings, are strongly affected by a tilting moment, a life which is around 10% shorter than that obtained with the Harris factor is to be expected. If the main wind direction is truly evenly spread over all compass directions, it is permissible to use the equivalent load of a ring that rotates relative to the load for the outer ring, approximately equivalent to simply using the Harris factor.

5 Conclusions

This work has given an overview of the literature on rolling contact fatigue calculation for oscillating bearings. Many approaches are based on ISO, tend to be user friendly, and are often applied in the literature. Most of these approaches have been proposed and used in the literature without an explanation as to when they apply. The aim of this paper was to explain when which approach can be applied. It is worth noting that many older publications, particularly for the Rumbarger effect and the Houpert effect, include errors or simplifications and hence more recent publications, including this one, are to be preferred as a source. When applied correctly according to more recent literature and for standard operating cases, the deviations between Harris, Rumbarger, and Houpert as well as other ISO-based approaches are typically not huge. This also applies to the operating conditions of pitch and yaw bearings. The large deviations obtained with alternative approaches to the Harris factor that are seen in some publications are often due to errors or simplifications. All ISO-based approaches shorten the calculated life compared to the results using the Harris factor (or are identical to it) if applied correctly.

Aside from these commonly used factors, a number of alternative approaches have been discussed. These include some ISO-related ones and some approaches that deviate significantly from ISO. Many of these alternative approaches, including ISO-related and non-ISO-related ones, have been designed particularly for rotor blade bearings.

The experimental validation of all models in the literature is relatively poor. Some results from the ISO-based approaches suggest that their predictions may be relatively close to the actual life, while validations of the alternative approaches are mostly lacking.

This work may help engineers identify which approach to use for the rolling contact fatigue life calculation for a given oscillating bearing. It has been written with a particular focus on wind turbine slewing bearings, but may also be used as a reference for any other oscillating bearings in other industrial sectors.

Appendix A: Derivation of the Rumbarger factor

Lundberg and Palmgren (1947) state, using Eq. 1 and knowing that $N = uL$,

$$\ln \frac{1}{S} \sim \frac{\tau_0^c (uL)^e}{z_0^h} V, \tag{A1}$$

where τ_0 is the maximum shear stress and z_0 its depth under the raceway, V is the loaded volume, and u gives the stress cycles per million oscillations or revolutions L. For a constant survival probability S, it follows that

$$L \sim \left(\frac{z_0^h}{\tau_0^c V} \right)^{1/e} u^{-1}. \tag{A2}$$

Comparing two identical bearings under identical τ_0 and z_0, one oscillating and one rotating, for $\theta < \theta_{\mathrm{crit}}$, where $V_{\mathrm{osc}}/V_{\mathrm{rot}} = \theta/\theta_{\mathrm{crit}}$ we obtain

$$a_{\mathrm{prt}} = \frac{L_{\mathrm{osc}}}{L_{\mathrm{rot}}} = \frac{u_{\mathrm{rot}}}{u_{\mathrm{osc}}} \left(\frac{\theta}{\theta_{\mathrm{crit}}} \right)^{-1/e}. \tag{A3}$$

500 This is equivalent to Eq. 18 given by Breslau and Schlecht (2020). In their Eq. 19, using θ_{crit} from Eq. 4, they then go on to derive[41]

$$a_{\mathrm{prt\,i,o}} = \frac{Z\left(1 \pm \gamma\right)}{4} \left[\frac{\theta Z\left(1 \pm \gamma\right)}{360°} \right]^{-1/e} \tag{A4}$$

with the minus $(-)$ sign referring to the outer and the plus $(+)$ sign to the inner raceway. Using a_{Harris} from Eq. 3, this can be rewritten as done by Houpert and Menck (2021)

505 $$a_{\mathrm{prt\,i,o}} = \left(\frac{\theta}{\theta_{\mathrm{crit\,i,o}}} \right)^{1-1/e} a_{\mathrm{Harris}}. \tag{A5}$$

Both Rumbarger and the NREL DG03 (co-authored by Rumbarger) use a different amplitude definition than in this paper, defined by $\varphi = 2\theta$. Equation A4 then becomes

$$a_{\mathrm{prt\,i,o}} = \frac{Z\left(1 \pm \gamma\right)}{4} \left[\frac{\varphi Z\left(1 \pm \gamma\right)}{720°} \right]^{-1/e} \tag{A6}$$

$$= \underbrace{\left(1 \pm \gamma\right)^{1-1/e} 4^{-1+1/e}}_{f_{\mathrm{Rum}}} Z^{1-1/e} \left[\frac{\varphi}{180°} \right]^{-1/e}. \tag{A7}$$

510 The factor f_{Rum} is introduced here to include the terms $(1 \pm \gamma)$ and $4^{-1+1/e}$, both of which Rumbarger assumes to be approximately 1. Thus, Rumbarger obtains $f_{\mathrm{Rum}} \approx 1$. In order to keep track of the error introduced by this assumption, f_{Rum} will be retained in the following equations.

Rumbarger does not adjust life by using a factor, but by changing the load rating. A factor can be converted to an equivalent load rating using

515 $$L_{10,\mathrm{prt}} = a_{\mathrm{prt}} \left(\frac{C}{P} \right)^p = \left(\frac{a_{\mathrm{prt}}^{1/p} C}{P} \right)^p = \left(\frac{C_{\mathrm{Rum}}}{P} \right)^p \tag{A8}$$

with Eq. A7 used for the adjusted Rumbarger load rating

$$C_{\mathrm{Rum}} = a_{\mathrm{prt}}^{1/p} C = \left(f_{\mathrm{Rum}} Z^{1-1/e} \left[\frac{\varphi}{180°} \right]^{-1/e} \right)^{1/p} C. \tag{A9}$$

Equation A9 is identical to the load ratings given in (Rumbarger, 2003) and (Harris et al., 2009) when assuming $f_{\mathrm{Rum}} = 1$ and using the parameters given in Table A1.

520 The error can simply be corrected by using either Eq. A9 or Eq. A7 separately for each raceway (cf. Breslau and Schlecht (2020)) and without assuming $f_{\mathrm{Rum}} = 1$.

---

[41]Equations here are adjusted to use degrees rather than radians as done in the reference.

[42]Exponent $p = 4$ follows from the given c, e, and h, and is consequently used by Rumbarger (2003) as well as Breslau and Schlecht (2020) in their derivations. Nonetheless, ISO 281 uses $p = 10/3$ in calculating $L = \left(\frac{C}{P} \right)^p$. This is explained in (Lundberg and Palmgren, 1952) and (ISO, a), which argue

Table A1. Exponents c, e, h, p according to ISO

	c	e	h	p
Point contact (ball bearings)	31/3	10/9	7/3	3
Line contact (roller bearings)	31/3	9/8	7/3	4 or[42] 10/3

Appendix B: Error of the Rumbarger factor for $\theta < \theta_{\mathrm{crit}}$

By assuming $(1 \pm \gamma) \approx 1$, Rumbarger effectively neglects the difference between inner and outer races and obtains an equation which can be used for the entire bearing. The assumption $4^{-1+1/e} \approx 1$, on the other hand, is an unnecessary simplification that leads to errors, as will be seen in the following.

B1 Error on one raceway

The error of Rumbarger's assumptions for one single raceway can be easily calculated by comparing the life $L_{10,\mathrm{prt}}$ from Eq. A8 that, correctly, assumes $f_{\mathrm{Rum}} \neq 1$ to that which approximates $f_{\mathrm{Rum}} = 1$ as done by Rumbarger.

$$\frac{L_{10,\mathrm{prt}}(f_{\mathrm{Rum}} = 1)}{L_{10,\mathrm{prt}}(f_{\mathrm{Rum}} \neq 1)} = \frac{1}{f_{\mathrm{Rum}}} \tag{B1}$$

Values of $1/f_{\mathrm{Rum}}$ for point and line contact as well as different values of γ are depicted in Fig. B1. One can see that C_{Rum} consistently overestimates the actual life, up to 23% for $\gamma = 0.35$ on a roller bearing's outer ring. The error is dominated by Rumbarger's neglect of the factor $4^{-1+1/e}$, which is 0.87 for point contact and 0.86 for line contact. Simply assuming $\gamma = 0$ thus causes an error of roughly 15% to 17%. Further differences are caused by neglecting $(1 \pm \gamma)^{1-1/e}$, which appears reasonable for very large bearings ($\gamma \to 0$) but less so for smaller ones ($\gamma \gg 0$).

B2 Error for the entire bearing

For the entire bearing, the matter is more complex. Adjusted lives $L_{\mathrm{prt\,i}} = a_{\mathrm{prt\,i}} L_{\mathrm{i}}$ of the inner ring and $L_{\mathrm{prt\,o}} = a_{\mathrm{prt\,o}} L_{\mathrm{o}}$ of the outer one can be combined via

$$L_{\mathrm{prt}} = \left(L_{\mathrm{prt\,i}}^{-e} + L_{\mathrm{prt\,o}}^{-e} \right)^{-1/e}. \tag{B2}$$

For an axial bearing with $\gamma = 0$ giving $a_{\mathrm{prt\,i}} = a_{\mathrm{prt\,o}}$ and $L_{\mathrm{i}} = L_{\mathrm{o}}$ this can be simplified into

$$L_{\mathrm{prt}} = 2^{-1/e} a_{\mathrm{prt\,i}} L_{\mathrm{i}}. \tag{B3}$$

---

for the choice of $p = 10/3$ because in some load cases, line contact within roller bearings may turn into point contact. Thus: $p = 4$ for detailed calculations of rolling contact fatigue where line contact is sure to take place; and $p = 10/3$ for calculations by general users applying $(C/P)^p$.
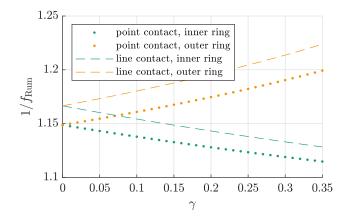
WIND
ENERGY
SCIENCE
DISCUSSIONS

Figure B1. $\frac{L_{10,\text{prt}}(f_{\text{Rum}}=1)}{L_{10,\text{prt}}(f_{\text{Rum}}\neq 1)}$ for inner and outer ring with point and line contact.

The relative difference between assuming $f_{\text{Rum}} = 1$ and $f_{\text{Rum}} \neq 1$ is then again given by $L_{\text{prt}}(f_{\text{Rum}} = 1)/L_{\text{prt}}(f_{\text{Rum}} \neq 1) = 1/f_{\text{Rum}}$, thus giving the same deviations as Fig. B1 for $\gamma = 0$. If $\gamma \neq 0$, the errors will deviate depending on the specific bearing design.

Appendix C: Extension of the Rumbarger effect for unevenly loaded volume with $\theta > \theta_{\text{crit}}$

545   For the operational scenario shown in Fig. 4 in yellow, the volume may be separated into volumes ψ_1 and ψ_2 each experiencing one or two stress cycles per oscillation, with $\psi_1 + \psi_2 = 360°/Z$. The corresponding oscillation amplitudes are given by $\theta_{\psi_1} + \theta_{\psi_2} = \theta_{\text{crit}}$, where $\theta_{\psi_2} = \theta - \theta_{\text{crit}}$. Equation A4 may then be used separately for each of the individual volumes to obtain $L_{\psi_1} = a_{\text{prt},\psi_1}L$ and the overlapping volume ψ_2 experiencing twice as many cycles, giving $L_{\psi_2} = \frac{1}{2}a_{\text{prt},\psi_2}L$. These can be combined via

$$L_{\psi_1+\psi_2} = \left(L_{\psi_1}^{-e} + L_{\psi_2}^{-e} \right)^{-1/e} \tag{C1}$$

$$= \underbrace{\left(a_{\text{prt},\psi_1}^{-e} + \left(\frac{1}{2}a_{\text{prt},\psi_2} \right)^{-e} \right)^{-1/e}}_{a_{\text{prt},\psi_1+\psi_2}} L. \tag{C2}$$

This allows for the analysis of the Rumbarger effect for oscillations $\theta > \theta_{\text{crit}}$ with overlapping volumes. Fig. C1 shows an exemplary calculation of $a_{\text{prt},\psi_1+\psi_2}$ for a 7220 type bearing normalized to the Harris factor. The result of $a_{\text{prt},\psi_1+\psi_2}$ can be seen to be almost identical to a_{Harris}.

555   *Author contributions.* OM: Conceptualization, Investigation, Writing - original draft preparation, Data curation, Software, Visualization; MS: Investigation, Writing - review & editing, Supervision
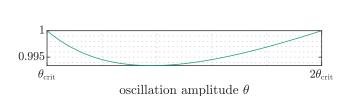
Figure C1. $a_{\mathrm{prt},\alpha+\beta}/a_{\mathrm{Harris}}$ for the inner ring of a 7220 type bearing for $\theta > \theta_{\mathrm{crit}}$.

References

Ermüdungslebensdauer von Wälzlagern unter Schwenkbewegungen, vol. Forschungsvorhaben 824, Frankfurt, 2021.

Stillstehende fettgeschmierte Wälzlager, vol. Forschungsvorhaben Nr. 540 III, Frankfurt, 2022.

ASTM: ASTM E1049-85(2017): Standard Practices for Cycle Counting in Fatigue Analysis, https://doi.org/10.1520/E1049-85R17, 2017.

Behnke, K. and Schleich, F.: Exploring Limiting Factors of Wear in Pitch Bearings of Wind Turbines with Real Scale Tests, https://doi.org/10.5194/wes-2022-96, 2022.

Breslau, G. and Schlecht, B.: A Fatigue Life Model for Roller Bearings in Oscillatory Applications, Bearing World Journal, pp. 65–80, https://d-nb.info/1233208187/34#page=65, 2020.

de La Presilla, R., Wandel, S., Stammler, M., Grebe, M., Poll, G., and Glavatskih, S.: Oscillating rolling element bearings: A review of tribotesting and analysis approaches, Tribology International, 188, 108 805, https://doi.org/10.1016/j.triboint.2023.108805, 2023.

Decker, K.-H.: Maschinenelemente, Das Fachwissen der Technik, Hanser, München, 12., überarb.u. erw. aufl. edn., 1995.

Dominik, W. K.: Rating and Life Formulas for Tapered Roller Bearings, in: SAE Technical Paper Series, SAE Technical Paper Series, SAE International400 Commonwealth Drive, Warrendale, PA, United States, https://doi.org/10.4271/841121, 1984.

Escalero, M., Olave, M., Behnke, K., and Muñiz-Calvente, M.: iKonPro®: A software for the probabilistic prediction of rolling contact fatigue, in publication, 2023.

Grebe, M.: False-Brinelling und Stillstandsmarkierungen bei Wälzlagern: Schäden bei Vibrationsbelastung oder kleinen Schwenkwinkeln, vol. 703. TAE of *Kontakt & Studium*, expert verlag, Renningen, https://doi.org/3351, 2017.

Haberhauer, H. and Bodenstein, F.: Maschinenelemente: Gestaltung, Berechnung, Anwendung: mit 108 Tabellen, Springer-Lehrbuch, Springer, Berlin and Heidelberg, 11., vollst. überarb. aufl. edn., 2001.

Hai, G. X., Diao, H. X., Jing, H. R., Hua, W., and Jie, C.: A Rolling Contact Fatigue Reliability Evaluation Method and its Application to a Slewing Bearing, Journal of Tribology, 134, https://doi.org/10.1115/1.4005770, 2012.

Harris, T., Rumbarger, J. H., and Butterfield, C. P.: Wind Turbine Design Guideline DG03: Yaw and Pitch Rolling Bearing Life, https://doi.org/10.2172/969722, 2009.

Harris, T. A.: Rolling Bearing Analysis, 4th Edition, John Wiley & Sons, Inc., 2001.

Harris, T. A. and Kotzalas, M. N.: Rolling Bearing Analysis, 5th Edition, Taylor & Francis, Boca Raton, 2007.

Houpert, L.: Bearing Life Calculation in Oscillatory Applications©, Tribology Transactions, 42, 136–143, https://doi.org/10.1080/10402009908982200, 1999.

Houpert, L. and Menck, O.: Bearing life calculations in rotating and oscillating applications, Journal of Tribology, pp. 1–31, https://doi.org/10.1115/1.4052962, 2021.

Hwang, J.-I.: Damage accumulation based fatigue life prediction of rolling bearings, Dissertation, Gottfried Wilhelm Leibniz University Hannover, Hanover, 2023.

Hwang, J.-I. and Poll, G.: A new approach for the prediction of fatigue life in rolling bearings based on damage accumulation theory considering residual stresses, Frontiers in Manufacturing Technology, 2, https://doi.org/10.3389/fmtec.2022.1010759, 2022.

IEC: Wind turbines - Part 1: Design requirements, 2019.

ISO: ISO/TR 1281-1:2008 + Cor. 1:2009: Rolling bearings — Explanatory notes on ISO 281 — Part 1: Basic dynamic load rating and basic rating life , a.

ISO: ISO/TR 1281-2:2008(E) - Rolling bearings — Explanatory notes on ISO 281 — Part 2: Modified rating life calculation, based on a systems approach to fatigue stresses, b.

ISO: ISO/TS 16281:2008 + Cor. 1:2009: Rolling bearings – Methods for calculating the modified reference rating life for universally loaded bearings , c.

600 ISO: ISO 281:2007: Rolling bearings – Dynamic load ratings and rating life, d.

Keller, J. and Guo, Y.: Rating of a Pitch Bearing for a 1.5-Megawatt Wind Turbine, https://doi.org/10.2172/1902646, 2022.

Leupold, S., Schelenz, R., and Jacobs, G.: Method to determine the local load cycles of a blade bearing using flexible multi-body simulation, Forschung im Ingenieurwesen, 85, 211–218, https://doi.org/10.1007/s10010-021-00457-y, 2021.

Liebherr-Components AG: Product Catalogue Slewing Bearings, 2017.

605 Lopez, A., Zurutuza, A., Olave, M., Portugal, I., Muñiz-Calvente, M., and Fernandez-Canteli, A.: Pitch bearing lifetime prediction considering the effect of pitch control strategy, Journal of Physics: Conference Series, 1222, 012 017, https://doi.org/10.1088/1742-6596/1222/1/012017, 2019.

Lundberg, G. and Palmgren, A.: Dynamic Capacity of Rolling Bearings: Proceedings of the Royal Swedish Adademy of Engineering Sciences, 196, Generalstabens Litografiska Anstalts Förlag, Stockholm, 1947.

610 Lundberg, G. and Palmgren, A.: Dynamic Capacity of Roller Bearings: Proceedings of the Royal Swdish Adademy of Engineering Sciences, 210, Generalstabens Litografiska Anstalts Förlag, Stockholm, 1952.

Menck, O.: The Finite Segment Method—A Numerical Rolling Contact Fatigue Life Model for Bearings Subjected to Stochastic Operating Conditions, Journal of Tribology, 145, https://doi.org/10.1115/1.4055916, 2023.

Menck, O., Stammler, M., and Schleich, F.: Fatigue lifetime calculation of wind turbine blade bearings considering blade-dependent load

615 distribution, Wind Energy Science, 5, 1743–1754, https://doi.org/10.5194/wes-5-1743-2020, 2020.

Menck, O., Behnke, K., Stammler, M., Bartschat, A., Schleich, F., and Graßmann, M.: Measurements and modeling of friction torque of wind turbine blade bearings, Journal of Physics: Conference Series, 2265, 022 087, https://doi.org/10.1088/1742-6596/2265/2/022087, 2022.

Münzing, T.: Auslegung von Kugelgewindetrieben bei oszillierenden Bewegungen und dynamischer Belastung, Dissertation, Universität Stuttgart, Stuttgart, https://doi.org/10.18419/opus-9601, 2017.

620 Rezaei, A., Guo, Y., Keller, J., and Nejad, A. R.: Effects of wind field characteristics on pitch bearing reliability: a case study of 5 MW reference wind turbine at onshore and offshore sites, Forschung im Ingenieurwesen, 87, 321–338, https://doi.org/10.1007/s10010-023-00654-x, 2023.

Roloff, H., Matek, W., and Wittel, H.: Maschinenelemente: Normung, Berechnung, Gestaltung, Viewegs Fachbücher der Technik, Vieweg, Braunschweig, 11., durchges. aufl. edn., 1987.

625 Rumbarger, J. H.: Simplification of Dynamic Capacity and Fatigue Life Estimations for Oscillating Rolling Bearings, Journal of Tribology, 125, 868–870, https://doi.org/10.1115/1.1576424, 2003.

Rumbarger, J. H. and Jones, A. B.: Dynamic Capacity of Oscillating Rolling Element Bearings, Journal of Lubrication Technology, 90, 130–138, https://doi.org/10.1115/1.3601528, 1968.

Sadeghi, F., Jalalahmadi, B., Slack, T. S., Raje, N., and Arakere, N. K.: A Review of Rolling Contact Fatigue, Journal of Tribology, 131,

630 https://doi.org/10.1115/1.3209132, 2009.

Schaeffler Technologies AG & Co. KG: Rolling bearings, Catalogue (HR 1): order number 029679141-0000, 2019.

Schmelter, R.: Über die Lebensdauerberechnung oszillierender Wälzlager, https://www.imw.tu-clausthal.de/fileadmin/Forschung/InstMitt/ 2011/_1.Artikel_8_35_rs_Beruecksichtigung_oszillatorischer_Rotation_bei_der_Auslegung_von_Waelzlagern_.pdf, 2011.

Schwack, F.: Untersuchungen zum Betriebsverhalten oszillierender Wälzlager am Beispiel von Rotorblattlagern in Windenergieanlagen, Dissertation, Leibniz University Hannover, https://doi.org/10.15488/9756, 2020.

Schwack, F., Stammler, M., Poll, G., and Reuter, A.: Comparison of Life Calculations for Oscillating Bearings Considering Individual Pitch Control in Wind Turbines, Journal of Physics: Conference Series, 753, 112 013, https://doi.org/10.1088/1742-6596/753/11/112013, 2016.

Stammler, M.: Endurance test strategies for pitch bearings of wind turbines, Dissertation, Leibniz University Hannover, https://doi.org/10.15488/10080, 2020.

Stammler, M., Reuter, A., and Poll, G.: Cycle counting of roller bearing oscillations – case study of wind turbine individual pitching system, Renewable Energy Focus, 25, 40–47, https://doi.org/10.1016/j.ref.2018.02.004, 2018.

Tallian, T. E.: Simplified Contact Fatigue Life Prediction Model—Part I: Review of Published Models, Journal of Tribology, 114, 207–213, https://doi.org/10.1115/1.2920875, 1992.

Tawresey, J. S. and Shugarts, W. W., Jr.: An Experimental Investigation of the Fatigue Life and Limit Load Characteristics of Needle Roller Bearings Under Oscillating Load Conditions, https://apps.dtic.mil/sti/citations/AD0437467, 1964.

Wenske, J., ed.: Wind turbine system design: Volume 1, nacelles, drive trains and verification, vol. 142A of *IET energy engineering series*, The Institution of Engineering and Technology, London and Stevenage, https://doi.org/10.1049/PBPO142F, 2022.

Wöll, L., Jacobs, G., and Kramer, A.: Lifetime Calculation of Irregularly Oscillating Bearings in Offshore Winches, Modeling, Identification and Control: A Norwegian Research Bulletin, 39, 61–72, https://doi.org/10.4173/mic.2018.2.2, 2018.